Journal of the European Ceramic Society 19 (1999) 2349–2357

PII: S0955-2219(99)00111-9
0955-2219/99/$ - see front matter

New Developments in α-SiAlON Ceramics

Hasan Mandal

Department of Ceramics Engineering, Anadolu University, 26470, Eskisehir, Turkey

Abstract

Two different α-sialon compositions have been densified by either pressureless sintering or capsul-free sinter HIPing using either single cation namely strontium, lanthanum, cerium, neodymium or their equimolar mixtures with calcium/ytterbium as a principal cation. The resulting materials have been heat-treated at 1450 °C for a maximum of 720 h to observe the α → β sialon transformation. Effect of starting compositions on the phase stabilities, microstructure, room temperature mechanical properties and optical transparent nature of sintered materials have been investigated. SEM observations for oxygen rich starting compositions revealed that α-sialon grains exist in needle like morphology in all the systems studied after both pressureless sintering and HIPing. Suprisingly, the nitrogen rich starting compositions give rise to coloured, optically transparent α-sialon ceramics after capsul-free HIPing. Clear evidence of α-sialon formation with incorporation of large cations namely, La^{3+}, Ce^{3+}, Nd^{3+} and Sr^{2+}, has been established by XRD, SEM and EDX analysis. The observed phenomenon could possibly extend the usefulness of α-sialons ceramics to both structural and functional applications.

Keywords: hot isostatic pressing, sintering, microstructure-final, mechanical properties, optical properties, sialon.

1 Introduction

Sialon ceramics have been developed for structural engineering applications. They offer advantages of easier fabrication compared with Si_3N_4 ceramics because of the lower viscosity of the M-Si-Al-O-N liquid phase, where M is one of the cations Li, Mg, Ca, Y, Sc and most rare earths, which facilitates easier densification at sintering temperatures.

β-Sialons, which are the first developed group in the sialon materials, are formed by substituting up to two-thirds of the Si in the β-Si_3N_4 by Al provided that valency compensation is maintained by the replacement of an equivalent concentration of N by O to give a range of β-sialons, $Si_{6-z}Al_zO_zN_{8-z}$ with $0 < z < 4$. Thus, z (Si–N) bonds are replaced by z (Al–O) bonds. Since the difference between the respective bond lengths (1·74 Å for Si–N and 1·75 Å for Al–O) is small, the lattice strain is also small and the extent of replacement is wide. Monolithic β-sialon materials can be easily densified by pressureless sintering since the presence of alumina in the starting mix lowers the eutectic temperature of the densifying liquid phase by some 200–300 °C. The resulting β-sialon materials possess a high degree of toughness (8 $MPam^{1/2}$) by *in situ* reinforcement with the elongated β-sialon grains. They also possess good strength up to 1000 MPa and excellent thermal shock resistance.[1]

α-Sialons were first observed very shortly after β-sialons with the general formula $M_xSi_{12-m-n}Al_{m+n}O_nN_{16-n}$, where M is one of the cations Li, Mg, Ca, Y and most rare earths (excluding La, Ce, Pr and Eu). x is equal to m divided by the valency of the M cation; there is a minimum value for the x parameter (0·3–0·5; i.e. there is an immiscibility gap between α-Si_3N_4 and α-sialon phases) and x can not exceed 2 since there are only two interstitial sites in each unit cell. In α-sialons, m (Si–N) bonds (1·74 Å) are replaced by the much longer Al–N (1·87 Å) and n (Si–N) bonds are replaced by similar sized Al–O (1·75 Å). The larger lattice strain resulting from the replacement of Si–N by Al–N restricts the range of solid solution (m-value) in α-sialon compared with β-sialon. The n-value is also restricted because high values are expected to favour β-sialon formation.[2]

Studies by Ekström and co-workers[3] on the sintering of α-sialon ceramics showed that the largest rare-earth cation to enter the α-sialon structure alone is Nd^{3+}, with an ionic radius around 0·99 Å. The same authors[4] also claimed for the slightly larger cation Ce^{3+}, with a radius of 1·03 Å, could not enter the α-sialon structure alone, but may enter when mixed with a smaller stabilizing cation

like Y^{3+} (radius 0·89Å). Similar observations were also made by Hwang *et al.*,[5] in Sr^{2+} (radius 1·26 Å) doped samples. Their reports indicate that Sr^{2+} alone did not form an -sialon but it could be accommodated into α-sialon structure only in conjunction with Ca^{2+} and Y^{3+}. No evidence, however, has been found for the incorporation of La^{3+} (radius 1·06 Å), largest rare earth cation, into the α-sialon structure even if added together with yttrium.[6] More recently, Mandal and Thompson[7] showed that α-sialon can be doped with only Ce^{3+} by quenching at a rate of 600 °C/min from sintering temperature at 1800 °C.

An important advantage of α-sialons is that the amount of intergranular phase is reduced by the transient liquid phase being absorbed into the matrix α-sialon phase during sintering. Another advantage is that the final product shows increased hardness. However, fracture toughness of α-sialon is poor relative to β-sialon and β-Si_3N_4 as α-sialon is generally observed in the form of equiaxed grains. It is also important to note that full densification can only be achieved either by hot pressing or capsul HIPing.

α and β-sialon phases are completely compatible and α-sialon/β-sialon composites are readily prepared by a single stage sintering of the appropriate mixture of nitrides and oxides. Therefore, in recent years, mixed α–β sialon materials have received increasing attention because of their easier fabrication compared with Si_3N_4 ceramics. More importantly, because good mechanical properties can be obtained due to the high hardness of α-sialon and the good strength and toughness of β-sialon.[8,9] However, the hardness and toughness of the α–β composites are not as high as their monolithic counterparts. Moreover, it has recently been found that the phase composition and microstructure of α- and α–β sialon ceramics are greatly affected by post sintering heat treatment procedures at lower temperatures (1300–1600 °C) when rare earth oxides are used as sintering additives. The α-sialon phase is only stable at high temperatures and transforms to β-sialon plus other crystalline or vitreous phases.[10–12] The ease with which this transformation proceeds decreases with increasing atomic number of the rare earth cation; indeed, in the absence of β-sialon nuclei, certain ytterbium α-sialon compositions do not transform to β even when high levels of liquid phase are present.[13,14] This transformation provides a convenient mechanism for controlling the mechanical properties of the final material. However, it can only be used beneficially in applications where the maximum service temperature is below the transformation temperature (1000 °C) of the grain boundary glassy phase. High temperature properties, especially oxidation and creep resistance, significantly deteriorate above this temperature.

More recently, it has been proved that α-sialon ceramics can also be produced with elongated grain morphologies. First example for the elongated nature of α-sialon grains was observed by Hwang *et al.*,[5] using the mixture of CaO-SrO-Y_2O_3 as sintering additives. Similar observations were later found by Wang *et al.*,[15] and Shen *et al.*,[16] using CaO and rare earth oxides as sintering additives, respectively. More recently, Chen and Rosenflanz[17] showed improved fracture toughness in α-sialon ceramics sintered by using β-Si_3N_4 starting powder with rare earth oxides. They claimed elongated α-sialons could even be obtained with a small amount of grain boundary phase in nitrogen rich α-sialon starting compositions. They also showed that the fracture toughness value increases as the cation size of the rare earth dopant increases.

In the present work, densification of two different α-sialon starting compositions has been investigated by using either single cation namely strontium, lanthanum, cerium, neodymium, or their equimolar mixtures with calcium/ytterbium as a principal cation. The possibility of stabilization of large cations into the α-sialon structure have been explored. The resulting materials have been heat treated at 1450 °C for up to 720 h in order to observe the $\alpha \rightarrow \beta$ sialon transformation. Effect of starting compositions on the microstructure, room temperature mechanical properties and optical transparencies are discussed.

2 Experimental

Starting powder mixtures were prepared by using Si_3N_4, (UBE-E10), AlN (HC Starck-Berlin, Grade C), Al_2O_3 (Alcoa, Grade A16SG) together with M_xO_y (where M = Sr, Ca, La, Ce, Nd, Yb [99·9%, Alfa Rare Earth Products]) which acts as the densifying additives to give an overall -sialon composition with $m = 1{\cdot}25/n = 1{\cdot}15$ for composition 1 (C1) and $m = 1{\cdot}2/n = 2{\cdot}0$ for composition 2 (C2) (see Fig. 1). The added metal oxides were calcined at 800 °C for 4 h before use in order to remove volatile contents. While calculating the compositions, 1·4 wt% O and 1·6 wt% O (the manufacturer's specifications) present on the surfaces of Si_3N_4 and AlN respectively were taken into account. Powder mixtures were prepared by wet milling with ethanol as liquid medium using a planetary ball mill for 4 h in a sialon container and silicon nitride balls. The total amount of the prepared batch weighed 50 g. The milled slurries were dried at 40 °C in a rotary evaporator, resulting in weak agglomerates which could easily be passed through a 125 μm sieve. Specimens were compacted into pellets (about 5 g) by uniaxial pressing and then isostatical pressing

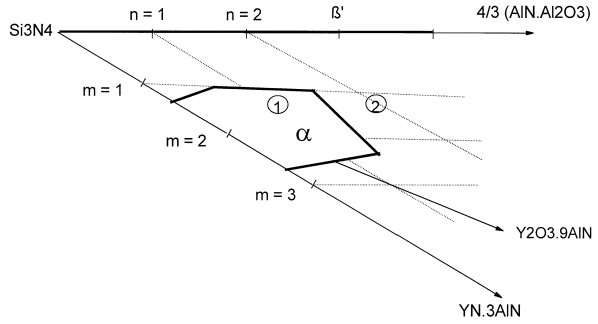

Fig. 1. α-Sialon plane showing the starting compositions used in this study. The α-sialon forming region for *Y* as mapped out by Sun *et al.*[18] is marked by the grey line.

with a pressure of 600 MPa. The green pellets were either pressureless sintered in a graphite resistance furnace (ASTRO) at 1800 °C for 2 h or capsul free sinter-HIPed in an ASEA QIH6 HIP-unit at 1800 °C (1·5 h at 1 MPa and 1·5 h at 50 MPa argon gas pressure) in a BN crucible or hot pressed (for certain compositions) in BN-coated graphite dies at 1800 °C for 1 h. Subsequent heat treatments were carried out for all samples in a molybdenum heating element furnace (ASTRO) at 1450 °C for up to 720 h (1 month) under nitrogen atmosphere. Product phases were characterised by X-ray diffraction (XRD) using a Siemens D500 diffractometer. Polished surfaces of sintered samples were examined in SEM (after carbon coating) using the back scattered mode attached with an energy dispersive X-ray analyser. Hardness and fracture toughness measurements were carried out at room temperature using a Vickers diamond indenter with 98 N (10 kg) load.

3 Results and Discussion

3.1 Formation of new α-sialons doped with large cations (Sr^{2+}, La^{3+}, Ce^{3+}, Nd^{3+})

Composition C1, $m = 1{\cdot}25$ and $n = 1{\cdot}15$, was selected for this study as it lies close to the minimum oxygen limit of α-sialon compositions. This enables exclusion of metal nitrides as starting compounds because of the cost involved and easy hydrolysing nature. α-sialon starting compositions with Nd-, Ce- and double-cation dopant additives were densified up to 99% of TD (theoretical density) by pressureless sintering and to 100% of TD by capsule-free sinter-HIPing (Table 1). In the case of only La_2O_3 and SrO additions, the densification was achieved exclusively by hot pressing since the pore closure could not be achieved after the first sintering stage, which is essential to obtain full density in the HIPing stage. SEM examination of polished cross-sections showed no porosity, indicating that the sample had virtually reached theoretical density.

X-ray examination of sintered samples showed that the cooling rate was sufficient to prevent crystallization of any grain boundary glass. The results of sintered and heat-treated samples are also given in Table 1. No α-sialon phase was observed in the case of only La_2O_3 and SrO additions. The sintered materials contained only β-sialon and a significant amount of the N-($La_3Si_8O_4N_{11}$) and S-(∼SrO1 ·$3Al_2O_30{\cdot}7Si_2N_2O$) phases. The reason for the chemical instability of La- and Sr- α-sialons can be explained in terms of ionic size i.e. there is a decreased tendency for $\alpha \rightarrow \beta$-sialon formation and increased tendency for the sialon transformation (see Section 3.2) with increase in the ionic radius of rare earth cations. However, in the case of only CeO_2 and Nd_2O_3 additions, approximately 50 and 100% α-sialon phases were obtained, respectively. These results also agree with the previous observation of Mandal and Thompson[7] that Ce^{3+} was the largest single cation ($r_{Ce3+} = 1{\cdot}03$ Å), which could enter the α-sialon structure alone. Samples densified with double cations, resulted in 100% of α-sialon as a matrix phase with minor amounts of 21R polytype after sintering. A typical

Table 1. Densities, phase analysis and α-sialon unit cell dimensions for the sintered samples in Cl [Measured densities of the HIPed samples were used as a theoretical density (TD)][a]

Sintering additive	*Density*	*XRD results (sintered)*	*Unit cell dimensions*		*XRD results (heat treated) (at 1450°C for 720 h)*
			a (Å)	*c (Å)*	
Nd_2O_3	%99·6	α-SiAlON, 21R	7·8280	5·6772	α-SiAlON, 21R, M′
CeO_2	%99·4	JEM, α-SiAlON, 21R	7·7858	5·6563	JEM,β-SiAlON, 21R
La_2O_3	HP	N-, β-SiAlON	no α-sialon		N-, β-SiAlON
SrO	HP	S-, β-SiAlON	no α-sialon		S-, β-SiAlON
Yb_2O_3-Nd_2O_3	%99·2	α-SiAlON, 21R	7·8109	5·6902	α-SiAlON, 21R, M′, J
Yb_2O_3-CeO_2	%99·0	α-SiAlON, 21R	7·7991	5·6698	α-SiAlON, 21R, JEM, J
Yb_2O_3-La_2O_3	%98·1	α-SiAlON, 21R	7·7878	5·6691	α-SiAlON, 21R, N, J
Yb_2O_3-SrO	%94·8	α-SiAlON, 21R	7·7997	5·6770	α-SiAlON, 21R, S, J,
CaO-Nd_2O_3	%94·5	α-SiAlON, 21R	7·8152	5·6906	α-SiAlON, 21R, M′
CaO-CeO_2	%98·5	α-SiAlON, 21R	7·8182	5·6782	α-SiAlON, 21R, JEM
CaO-La_2O_2	%97·0	α-SiAlON, 21R	7·7990	5·6665	α-SiAlON, 21R, N
CaO-SrO	%94·5	α-SiAlON, 21R	7·8088	5·6753	α-SiAlON, 21R, S

[a]JEM (∼$CeSi_5Al_2O_1N_9$); N ($La_3Si_8O_4N_{11}$); S(∼SrO1·$3Al_2O_30{\cdot}7Si_2N_2O$), M′ ($Nd_2Si_2AlO_4N_3$); J($Yb_4Si_2O_7N_2$)

back-scattered SEM images of the samples densified with CeO_2, $CaO\text{-}Nd_2O_3$, $CaO\text{-}La_2O_3$, are given in Fig. 2. Since the contrast on back scattered electron micrographs depends mainly on the mean atomic number, these micrographs clearly distinguish between various phases; 21R grains (which contain no sintering additive cation) appear black and more needle like, whereas the α-sialon grains (which contain a small amount of sintering additive cations) appear grey and more equiaxed whilst the crystalline or glassy phases(s) appear fine grained and white, because of the high cation content [in Fig. 2(a), large white agglomerates are JEM phase ($\approx CeSi_5Al_2ON_9$)]. The microstructures are homogeneous and consist of typical equiaxed α-sialon grains, except the $CaO\text{-}La_2O_3$ sample in which, a small amount of elongated α-sialon grains are also observed. Back scattered SEM images of CaO containing samples clearly indicate that La- and Nd- cations could be accommodated into the α-sialon structure, otherwise they should show only two phase regions: (1) α-sialon (doped only by Ca^{2+}) and 21R phases with dark grey colour and (2) grain boundary phases with bright colour (doped mainly by Nd^{3+} or La^{3+}). All sintered samples were analyzed by EDX, in point mode, to further prove that Ce-, La- and Sr- atoms have been incorporated into the α-sialon grains. EDX spectra for the corresponding samples are given in Fig. 3. The analysis of α-sialon grains carried out at different locations of the specimen show nearly identical results which clearly indicate that Sr^{2+}, La^{3+}, Ce^{3+} and Nd^{3+} cations have been incorporated into α-sialon grains with either Ca^{2+} or Yb^{3+}. The incorporation of these cations have also been supported by measurements of unit cell parameters (Table 1). It is highly plausible that, La^{3+} ($r = 1{\cdot}06$ Å) and Sr^{2+} ($r = 1{\cdot}26$ Å) do not form α-sialon on its own but form α-sialon phase with Ca^{2+} and Yb^{3+}. This can be explained in terms of (a) lower valency of Ca^{2+}, (and also Sr^{2+}) since the α-sialon stability increases with increasing cation solubility ($x = m/v$, v is the valency of cation), which, in turn increases with decreasing cation valency, (b) the mean size of multi-cations which well fit into the interstitial cation size in the α-sialon structure.

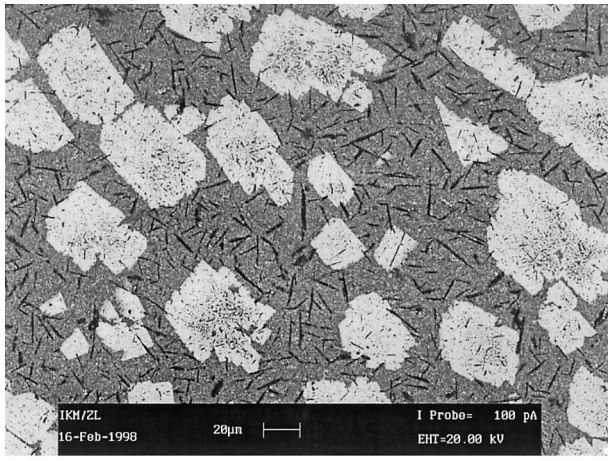

(a)

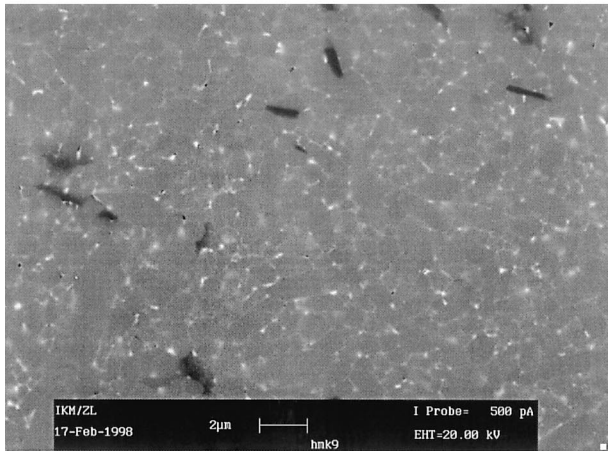

(b)

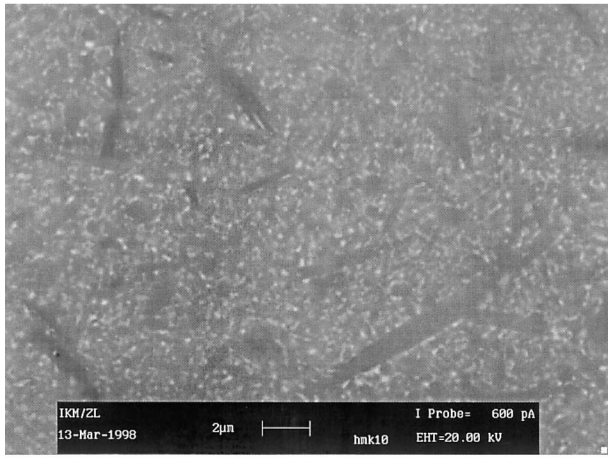

(c)

Fig. 2. Back-scattered SEM micrographs of the (a) CeO_2, (b) Nd_2O_3-CaO, (c) Nd_2O_3-Yb_2O_3 samples in C1, after sintering.

3.2 $\alpha \rightarrow \beta$ Sialon transformation

Subsequent prolonged heat treatments of sintered samples were carried out at 1450 °C in a nitrogen atmosphere up to 720 h (1 month) in order to study the effects of heat treatments on the $\alpha \rightarrow \beta$ sialon transformation and also the grain boundary crystallisation behaviour. In the heat treated SrO, La_2O_3 samples, the crystalline phases were the same as sintered ones but with an increasing amount of N- and S- phases.

In addition to the grain boundary crystallization, some of La-, Sr-, Ce-, Nd- and Yb- may be rejected on the heat treatment of α-sialon to give N-($La_3Si_8O_4N_{11}$), S-($\approx SrO1{\cdot}3Al_2O_30{\cdot}7Si_2N_2O$), JEM ($\approx CeSi_5Al_2O_1N_9$), M'($\approx Nd_2Si_2AlO_4N_3$), and J ($Yb_4Si_2O_7N_2$) phases, respectively. It is interesting to note that the residual α-sialon phases show no

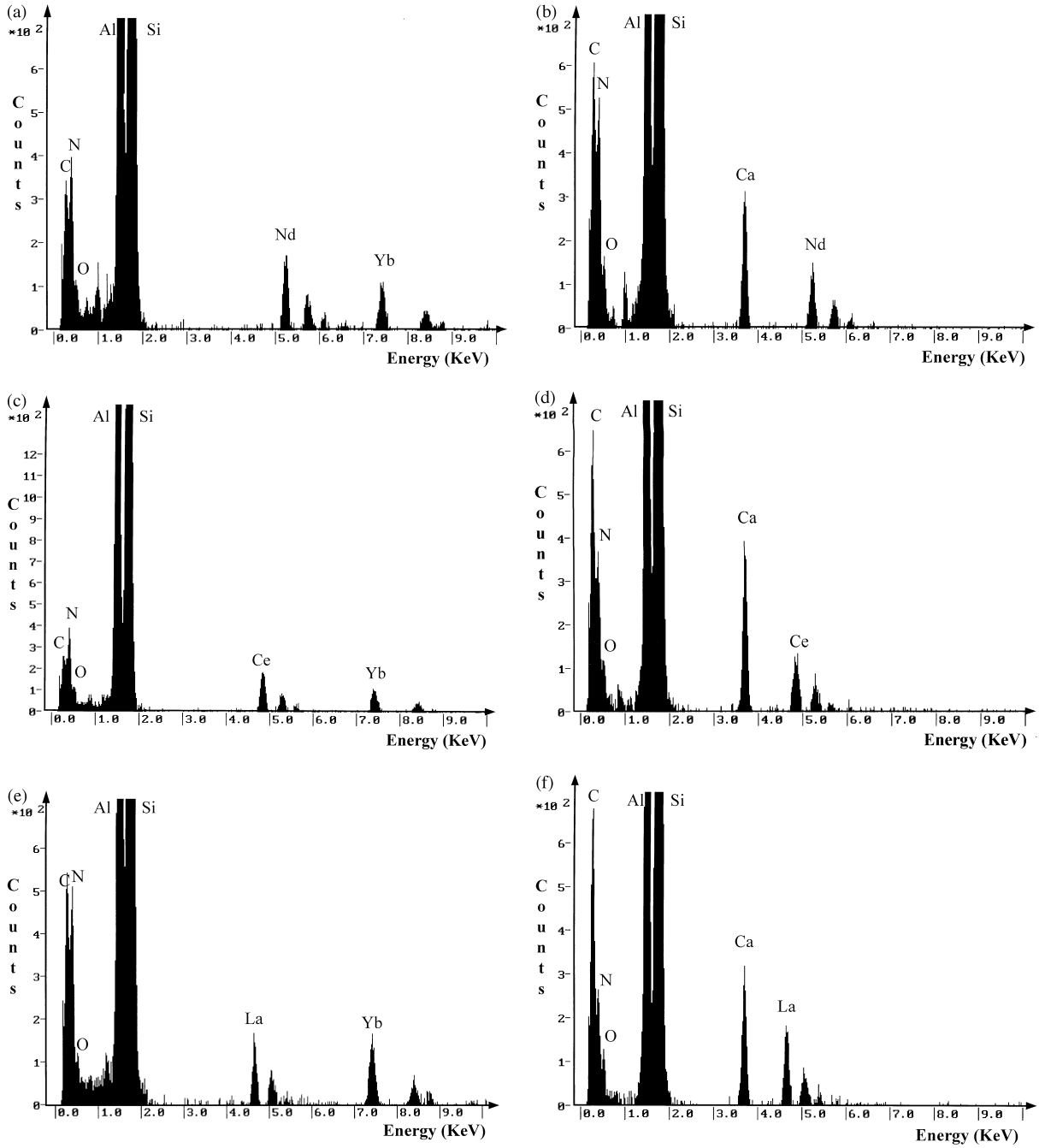

Fig. 3. EDX spectra for the sialon regions of (a) Nd_2O_3-Yb_2O_3, (b) Nd_2O_3-CaO, (c) CeO_2-Yb_2O_3, (d) CeO_2-CaO, (e) La_2O_3-Yb_2O_3, (f) La_2O_3-CaO samples in C1, after sintering.

transformation whatsoever to β-sialon even after 720 h (1 month) of heat treatment for the double-cation and Nd-doped materials (see Table 1). Back scattered SEM images and EDX spectra for all the samples, after heat treatments clearly prove that Sr-, La-, Ce-, Nd- cations remain inside the α-sialon grains. Only in the case of sole CeO_2 addition, the α-sialon gradually transformed to β-sialon + JEM phases and no α-phase was detected at all after 720 h heat treatment. More details of this work can be found elsewhere.[19]

Many results obtained in the present study are not consistent with conclusions previously deduced for rare earth stabilised α-sialon materials.[10–12] It is clear that α-sialons in which calcium or ytterbium is present jointly with large cation size rare earth elements do not undergo $\alpha \leftrightarrow \beta$ sialon transformation even when heat-treated at 1450 °C. This result confirms the increased size of the single-phase α-sialon phase-field in the calcium and ytterbium systems and also agree with the recent explanation given for $\alpha \leftrightarrow \beta$ sialon transformation, where the key factor is the transformation temperature ($T_{\alpha\beta}$), which not only varies with the sialon system but also with the composition within a system[20] and therefore $T_{\alpha\beta}$ increases with decreasing Z and increasing cation size; this is why a very rapid quench from 1800 °C is necessary in order to obtain even a small amount of Ce-α-sialon.[7] This explanation also gives an opportunity to

obtain only La-and Sr-doped α-sialons by quenching rapidly from sintering temperature.

3.3 α-sialon ceramics with elongated morphology

Another α-sialon starting composition (C2), which is outside the α-sialon forming region (according to Y_2O_3 system[18]), $m = 1{\cdot}2$ and $n = 2$, has been investigated either by using only Yb_2O_3, which is the smallest rare earth cation (0·865 Å), or equimolar mixtures of CaO-CeO_2 and CaO-Nd_2O_3, where Ce^{3+} (1·035 Å) and Nd^{3+} (0·995 Å) are the largest rare earths cations which can enter the α-sialon structure alone.

Table 2 gives densities and phase analysis (using XRD) after pressureless sintering. The major concern in densification of α-sialon materials by pressureless sintering is to choose an appropriate sintering additive that can stabilize the α-sialon structure and at the same time it should promote a transient liquid which can assist densification of the material. It can be seen from the table that all samples could easily be sintered to 100% of theoretical density even by pressureless sintering since the composition was rich in Al and O.

X-ray examination of sintered samples revealed that α-sialon was the only major phase coexisting with 21R polytypoid phase. It is difficult to explain why only α-sialon forms in these samples since the chosen composition does not lie inside the α-sialon forming region. This can be explained in terms of lower valency of Ca^{2+} since the α-sialon stability increases with increasing cation solubility ($x = m/v$, v is the valency of cation), which in turn, increases with decreasing cation valency, and also increasing the α-sialon formation region as decreasing the cation size of rare earth element. This result also confirms the divergence of the single-phase α-sialon phase-field in the calcium and ytterbium systems.

Figure 4(a) shows back scattered SEM image of the sample densified using Nd_2O_3-CaO resulted in elongated α-sialon grains with a high aspect ratio. Although the sintering additives, heating profile and crystalline phases were the same as in C1 (see Section 3.1), the morphology of α-sialon grains was found to be quite different. Similar features were also observed for CaO-CeO_2 and Yb_2O_3 doped α-sialons [Fig. 4(b) and (c)]. In the case of the Yb_2O_3 doped sample, the amount of α-sialon grains were relatively small with low aspect ratio.

The reason for the great difference between two compositions in terms of α-sialon grain morphologies

Table 2. %TD and crystalline phases in pressureless sintered samples. (Measured densities of the HIPed samples were used a theoretical density)

Sintering additive	*%TD*	*XRD results*
Composition 1 ($m = 1{\cdot}25$ and $n = 1{\cdot}15$)		
CaO-Nd_2O_3	%94·5	α-SiAlON, 21R
CaO-CeO_2	%98·5	α-SiAlON, 21R
Yb_2O_3	%69·2 [%71·1 (SHIP)]	α-SiAlON, 21R
Composition 2 ($m = 1{\cdot}2$ and $n = 2{\cdot}0$)		
CaO-Nd_2O_3	%100	α-SiAlON, 21R
CaO-CeO_2	%100	α-SiAlON, 21R
Yb_2O_3	%100	α-SiAlON, 21R

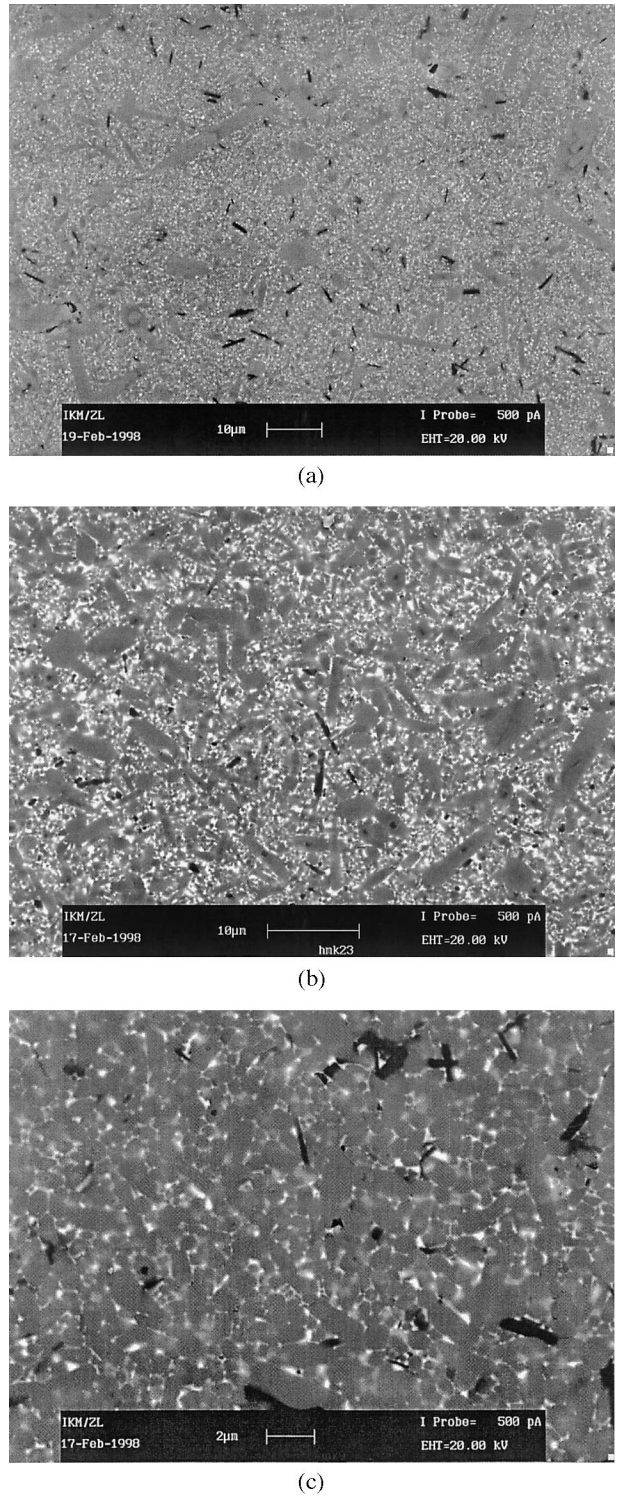

Fig. 4. Back-scattered SEM micrographs of the (a) Nd_2O_3-CaO, (b) CeO_2-CaO and (c) Yb_2O_3 samples in C2, after sintering.

can only be explained in terms of oxygen and aluminium contents (the amount of liquid phase appeared during sintering) of starting compositions. It could be possible that the presence of rare earth or calcium containing liquid phase during sintering favoured the growth of elongated α-sialon grains. The observation of lesser amount of elongated α-sialon grains in Yb_2O_3 doped sample [Fig. 4(c)] also confirms this statement.

Room temperature hardness (HV10) and indentation fracture toughness (K_{IC}) measurements for both compositions densified with Nd_2O_3-CaO additives are presented in Table 3. The hardness and toughness values for the sample in C1 is typical for α-sialon. However, the sample in C2 shows about 50% increase in toughness value compared to the C1 sample, which is typical for β-Si_3N_4 and β-sialon, while maintaining the hardness value of the C1 sample.

Figure 5 shows a crack propagation path for the above samples. Transgranular and intergranular crack propagations were observed for the sample with equiaxed grain morphology [Fig. 5(a)]. However, the crack propagation path for the samples with elongated α-grains show crack deflection, crack bridging and grain pull-out mechanisms [Fig. 5(b) and (c)] which resulted in improvement in fracture toughness value.

3.4 Translucent and coloured α-sialons

Research on α-sialon ceramics have been concentrated mostly on structural applications because of their high hardness and good thermal properties. Almost no attention has been paid to their functional applications. Recently, Karunaratne *et al.*[21] reported preparation of coloured α-sialon ceramic with relatively high optical transparency by careful control of the sintering atmosphere and adding suitable rare earths as stabilizing cations. The reason for this new phenomenon was explained in terms of change in valency state of the rare earth cation dopant. Hence, appearance was only seen in Yb- containing samples.

In this study, a wide range of coloured and translucent α-sialon ceramics have been obtained by capsul-free HIP sintering of samples in C1 [see Fig. 6, samples were not polished and their thicknesses vary up to 1000 μm (1 mm)]. The colour strongly depends on dopant rare earth oxide(s); i.e. gradient yellow (gradient depends on second dopant), violet, green, green-yellow, light yellow and grey for the ytterbium, neodymium, cerium, lanthanum-calcium, cerium-calcium and neodymium-calcium doped samples, respectively. Typical SEM microstructure for the translucent α-sialon was given in Fig. 7. However, no transparent samples were obtained with C2 (translucent only in polished surfaces and thin sections, 100 μm).

The observation for the optical transparency could possibly due to avoidance of intergranular material which can scatter light, (any contrast in

Table 3. Room temperature mechanical properties of Nd_2O_3-CaO doped α-sialons

Composition	K_{IC} *(MPa$^{1/2}$)*	*HV10 (GPa)*
1 (Equiaxed grains)	3·96	19·76
2 (Elongated grains)	6·31	19·30

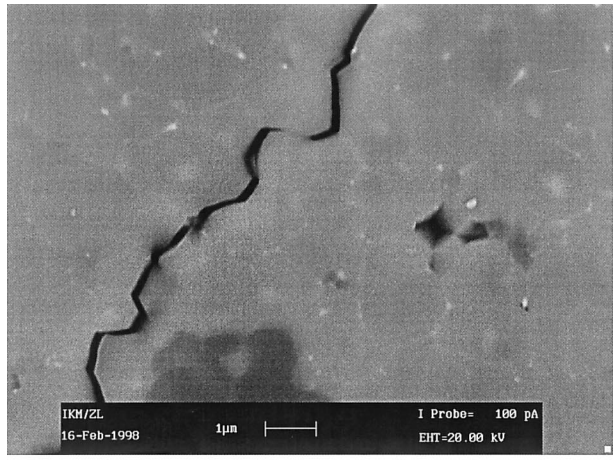

(a)

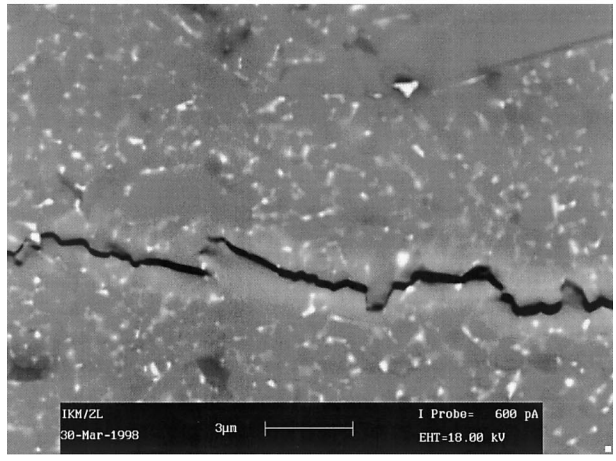

(b)

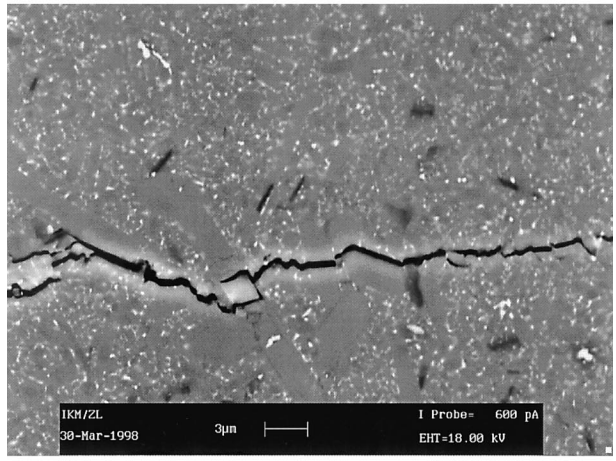

(c)

Fig. 5. Indentation crack trajectory of Nd_2O_3-CaO densified samples in (a) C1, (b) and (c) in C2.

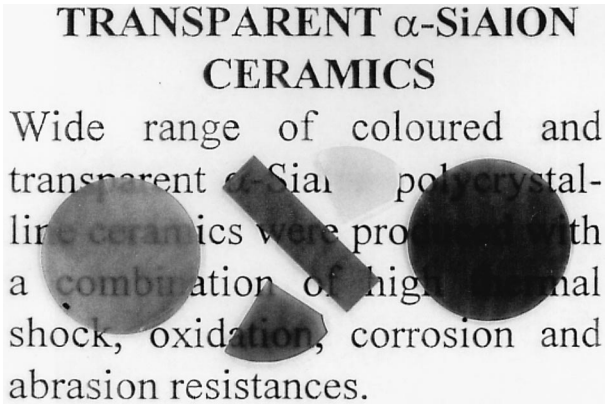

Fig. 6. Translucent α-sialon ceramics doped with (a) Nd_2O_3-CaO (grey-violet), (b) Nd_2O_3 (violet), (c) CeO_2-CaO (light yellow), (d) Nd_2O_3-Yb_2O_3 (yellow brown) after sintering and (e) sample (d), after heat treatment at 1450°C for 1 week.

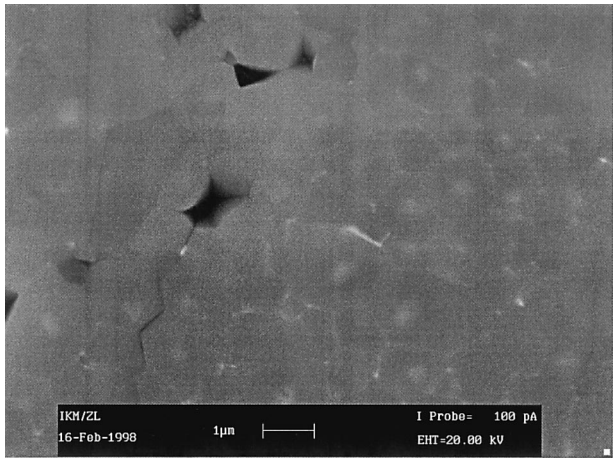

Fig. 7. Typical microstructure for a translucent α-sialon ceramic (doped with Nd_2O_3-CaO).

refractive index at a grain boundary will cause scattering) and the production of a single phase material, i.e. pure α-sialon (if both α and β sialon present, the slightly different refractive indices at grain boundaries will result in light scattering).

Heat treatment (at 1450 °C for 168 h) of these samples further improved the transparent nature [see Fig. 6(e)]. The oxidation test on sintered samples at various temperatures for 24 h show that the transparency can be maintained at temperatures as high as 1200 °C. Further details of this work are given in a separate publication.[22]

In comparison with already existing translucent ceramics, α-sialon has following superior properties: (a) high thermal shock resistance (compared to already found oxide based transparent materials), (b) high oxidation resistance (compared to already discovered non-oxide based transparent materials), (c) wide range of colours (compared to existing non-oxide based transparent materials). (d) shape selection (they can easily be sintered by capsul free sinter/HIPing). Therefore, this material may find itself useful as an abrasion resistant, tough window material with high resistance to oxidation and corrosion at elevated temperatures.

4 Conclusions

Densification and stabilization of α-sialon ceramics have been investigated by using oxides of large cations (Sr^{2+}, La^{3+}, Ce^{3+}, Nd^{3+}) and their equimolar mixtures with CaO or Yb_2O_3. All multication and single cation (only Nd^{3+} and Ce^{3+}) doped samples could be densified nearly to full densities even by pressureless sintering. X-ray diffraction on the samples densified with single cations revealed that α-sialon structure could accommodate Nd^{3+} or Ce^{3+} cations. In Sr- and La- systems, however, S-(~$SrO1{\cdot}3Al_2O_30{\cdot}7Si_2N_2O$) and N-($La_3Si_8O_4N_{11}$) phases were found to be more stable rather than α-sialon. In the case of multi-cations, α-sialon was observed as the only matrix phase. SEM, EDX, XRD measurements proved that Ce-, La- and Sr- cations could be accommodated into the α-sialon structure with the presence of calcium or ytterbium cations.

SEM studies on HIPed samples revealed that almost glass free grain boundaries can be obtained by careful design of starting compositions which resulted in high optical transparency.

In double cation doped α-β sialons, there was no $\alpha \rightarrow \beta$ transformation observed at 1450 °C in which Yb- or Ca- cations acted as a stabiliser to inhibit transformation.

α-Sialons with an elongated grain morphology have been developed in various sialon systems in oxygen and aluminium rich compositions. This type of morphology is more pronounced in oxides of large cation size rare earths (Nd^{3+} and Ce^{3+}) together with Ca^{2+}. Because of this, fracture toughness of the material has increased due to crack deflection, crack bridging and grain pull-out mechanisms. These new significant improvements in α-sialon ceramics may possibly widen the applicability of these ceramics not only to structural applications but also to functional applications.

Acknowledgements

It is a pleasure to thank Professor M. J. Hoffmann, Dr. R. Oberacker and Dr. P. D. Ramesh at Karlsruhe University, Professors K. H. Jack and Derek P. Thompson at Newcastle University, Dr. Y.-B. Cheng at Monash University, Dr. Z. J. Shen at Stockholm University, Dr. N. Camuscu at Kirikkale University who have contributed to some aspects of this work. I would also like to acknowledge financial assistance from the Alexander von

Humbolt Foundation (AvH, Germany) during the course of this work.

References

1. Jack, K. H., Review: sialons and related nitrogen ceramics. *J. Mater. Sci.*, 1976, **11**, 1135.
2. Hampshire, S., Park, H. K., Thompson, D. P. and Jack, K. H., α-Sialon ceramics. *Nature*, 1978, **274**, 880.
3. Ekström, T., Sialon ceramics sintered with yttria and rare earth oxides. In *Materials Research Society Symposium Proceedings*, ed. I-W. Chen, P. F. Becher, M. Mitomo, G. Petzow and T. S. Yen. MRS, Pittsburgh, 1993, pp.121.
4. Söderlund, E. and Ekström, T., Pressureless sintering of Y_2O_3-CeO_2 doped sialons. *J. Mater. Sci.*, 1990, **25**, 4815.
5. Hwang, C. J., Susintzky, D. W. and Beaman, D. R., Preparation of multication α-sialon containing strontium. *J. Am. Ceram. Soc.*, 1995, **78**, 588.
6. Olsson, P.-O. and Ekström, T., HIP-sintered β- and $\alpha - \beta$ sialons densified with Y_2O_3 and La_2O_3 additions. *J. Mater. Sci.*, 1990, **25**, 1824.
7. Mandal, H. and Thompson, D. P., CeO_2 doped α-sialon ceramics. *J. Mater. Sci. Lett.*, 1996, **15**, 1435.
8. Ekström, T. and Ingelström, I., Characterization and properties of sialon ceramics. In *Proceedings of the International Conference Non-Oxide Technical and Engineering Ceramics*, ed. S. Hampshire. Elsevier Applied Science Publishers. London, 1986, pp. 231.
9. Cao, G. Z., Metselaar, R. and Ziegler, G., Microstructure and properties of mixed $\alpha - \beta$ sialons. In *4th International Symposium on Ceramic Materials and Components for Engines*, ed. E. Carlsson, T, Johansson and L, Kahlman. Elsevier Applied Science Publishers, London, 1992, pp.188.
10. Mandal, H., Thompson, D. P. and Ekström, T., Reversible $\alpha \leftrightarrow \beta$ SiAlON transformation in heat treated sialon ceramics. *J. Eur. Ceram. Soc.*, 1993, **12**, 421.
11. Ekström, T. and Shen, Z. J., Temperature stability of rare earth doped α-sialon ceramics. In *5th Intern. Symp. on Ceramic Materials and Components for Engines*, ed. D. S. Yan, X. R. Fu and S. X. Shi. World Sci. Publ. Co., 1995, pp.206.
12. Zhao, R. and Cheng, Y.-B., Decomposition of Sm α-SiAlON phases during post-sintering heat treatment. *J. Eur. Ceram. Soc.*, 1996, **16**, 1001.
13. Camuscu, N., Thompson, D. P. and Mandal, H., Effect of starting composition, type of rare earth sintering additive and amount of liquid phase on $\alpha \leftrightarrow \beta$ sialon transformation. *J. Eur. Ceram. Soc.*, 1997, **17**, 599.
14. Mandal, H., Thompson, D. P, Liu, Q. and Gao, L., High temperature stability of α-sialon ceramics containing glass additions. *Eur. J. Solid. State. Inorg. Chem.*, 1997, **34**, 179.
15. Wang, H, Cheng, Y.-B., Muddle, C., Gao, L. and Yen, T. S., Preferred orientation in hot-pressed Ca α-sialon ceramics. *J. Mater. Sci. Lett.*, 1996, **15**, 447.
16. Shen, Z. J., Nordberg, L.-O., Nygren, M. and Ekström, T. α-Sialon grains with high aspect ratio-utopia or reality? In *Engineering Ceramics '96: Higher Reliability Through Processing*, ed. G. N. Babini, M. Havier and P. Sajgalik. Kluwer Academic Publications, The Netherlands, pp.199.
17. Chen, I.-W. and Rosenflanz, A., A tough sialon ceramic based on α-Si_3N_4 with a whisker-like microstructure. *Nature*, 1997, **389**, 701.
18. Sun, W. Y., Tien, T. Y. and Yen, T. S., Solubility limits of α'-sialon solid solutions in the system Si, Al, Y/N, O. *J. Am. Ceram. Soc.*, 1991, **74**, 2547.
19. Mandal, H., Hoffmann, M. J., Thompson D. P. and Jack, K. H., $\alpha \leftrightarrow \beta$ Phase transformation in multi-cation doped α-sialon ceramics. In *Proceedings of 9th CIMTEC World Congress, June, 1998*, Florence, Italy, in press.
20. Mandal, H., Thompson, D. P. and Jack, K. H., $\alpha \leftrightarrow \beta$ Phase transformations in silicon nitride and sialons. *Proceedings of International Symposium on Novel Synthesis and Processing of Ceramics Key Engineering Materials*, 1999, **159–60**, pp. 1.
21. Karunaratne, B. S. M., Lumby, R. J. and Lewis, M. H., Rare earth doped α-sialon ceramics with novel optical properties. *J. Mater. Res.*, 1996, **11**, 2790.
22. Mandal, H. and Hoffmann, M. J., Translucent α-sialon ceramics. In Preparation.